

Improvement of inspection system for common crossings by track side monitoring and prognostics

Mykola Sysyn^{*1}, Olga Nabochenko², Vitalii Kovalchuk²,
Dimitri Gruen¹ and Andriy Pentsak³

¹*Institute of Railway Systems and Public Transport, Technical University of Dresden, Dresden 01069, Germany*

²*Department of the rolling stock and track, Lviv branch of Dnipro National University of Railway Transport, Lviv 79052, Ukraine*

³*Department of Construction industry, Lviv Polytechnic National University, Lviv 79013, Ukraine*

(Received May 13, 2019, Revised July 15, 2019, Accepted July 17, 2019)

Abstract. Scheduled inspections of common crossings are one of the main cost drivers of railway maintenance. Prognostics and health management (PHM) approach and modern monitoring means offer many possibilities in the optimization of inspections and maintenance. The present paper deals with data driven prognosis of the common crossing remaining useful life (RUL) that is based on an inertial monitoring system. The problem of scheduled inspections system for common crossings is outlined and analysed. The proposed analysis of inertial signals with the maximal overlap discrete wavelet packet transform (MODWPT) and Shannon entropy (SE) estimates enable to extract the spectral features. The relevant features for the acceleration components are selected with application of Lasso (Least absolute shrinkage and selection operator) regularization. The features are fused with time domain information about the longitudinal position of wheels impact and train velocities by multivariate regression. The fused structural health (SH) indicator has a significant correlation to the lifetime of crossing. The RUL prognosis is performed on the linear degradation stochastic model with recursive Bayesian update. Prognosis testing metrics show the promising results for common crossing inspection scheduling improvement.

Keywords: railway common crossing; track-side monitoring; structural health indicator; MODWPT; Lasso regularization; RUL

1. Introduction

Reliability and availability of railway infrastructure depends on these of its main parts: signaling, catenary systems and engineering structures, as well as track infrastructure. The track infrastructure takes the most influencing part due to relatively short lifecycle of track superstructure elements. The lifecycle varies from about 20 years for rails and sleepers to 1 year for switch and crossing (S&C) elements (Lichtberger 2005). Therefore, track superstructure shares up to half of the overall maintenance costs of railway infrastructure (Lay and Rensing 2013). S&C is a critical element of railway infrastructure, not only because of its short lifecycle, but also due to the cost and time expensive maintenance. According to (Letot *et al.* 2013), almost 33% of the total

*Corresponding author, Ph.D., E-mail: mykola.sysyn@tu-dresden.de

maintenance costs of railway track are expended for maintenance of switches and crossings.

A common crossing with stiff frog is the most loaded part of switch due to a disruption of rolling contact surface. The most of common crossings on German railways (Zoll 2016) are assembled from rail steel R350 that is subjected to rail contact fatigue (RCF) damages, which usually limit the lifecycle of common crossing (EU Project INNOTRACK 2008). RCF failures of common crossing are developing not uniformly over the lifecycle, unlike the other crossing failures like rail wear, ballast settlements etc. The progress of RCF in common crossing rails accelerates during the lifetime and can be visually observed only after about three-quarters of the lifecycle. For that reason, the RCF failures are difficult to detect and predict with regular scheduled inspections. The explanation of influence of inspection intervals on time detection of RCF on common crossings is shown in Fig. 1.

The conventional scheduled inspections in railway infrastructure are usually planned based on the deterministic approach, where the inspection intervals should avoid the appearance of unexpected fault of track element with the mean lifecycle B_{mean} .

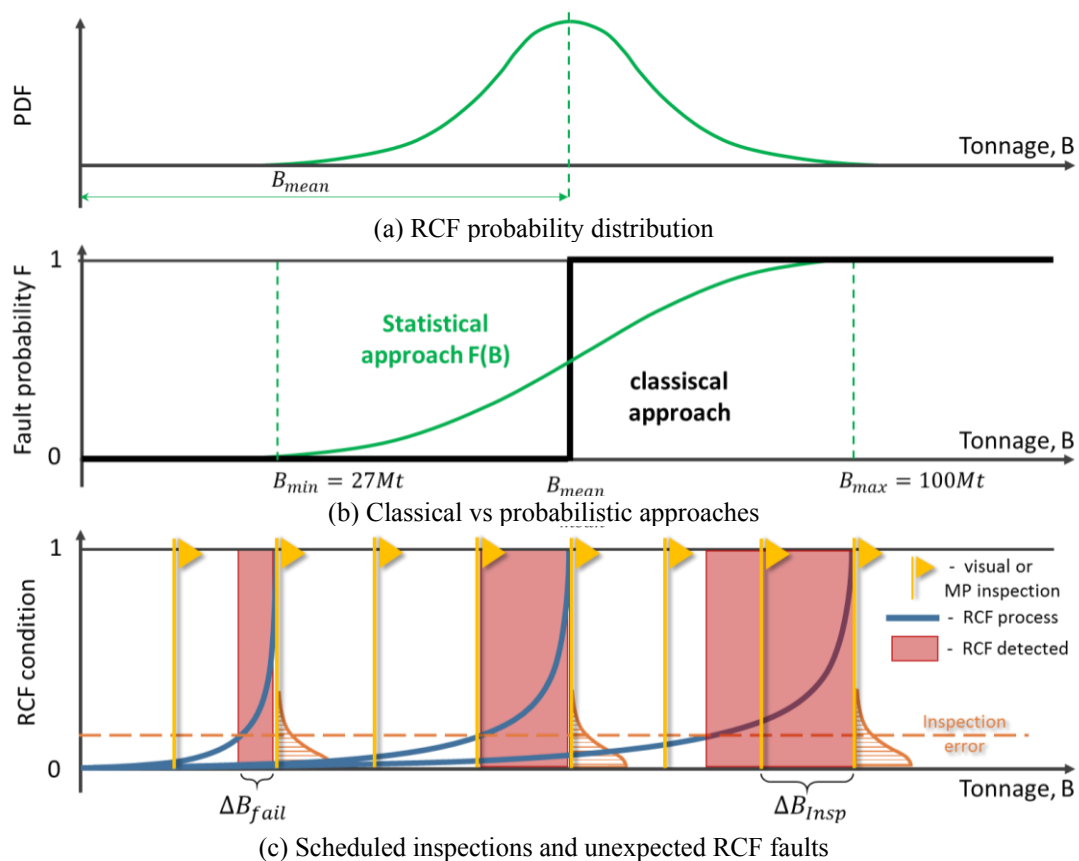


Fig. 1 Deterministic and probabilistic approach in the scheduled inspections planning (PDF - Probability density function; MP - Magnet particle)

However, the lifecycle of common crossing is characterized with a wide range between 27 Mt (Megatons) up to 100 Mt despite of the same type and materials for the similar operational loading (Gerber *et al.* 2015). The distribution of RCF fault probability is close to the normal one (Figs. 1(a) and 1(b)). The progress of RCF development for the short-, mean and long-living individuals of the distribution are shown in Fig. 1(c). It is usually considered as the exponential or the power law (Lichtberger 2005). The RCF can be positive true detected by visual inspections or by technical means, like magnet particle (MP) etc., with some error at the last RCF progress stage. If the RUL after detection ΔB_{fail} is less than the inspection interval ΔB_{Insp} , then the undetected RCF failures could appear. The unexpected RCF failures on common crossing rails can cause the unplanned maintenance works with long-term operational hindrance. The approximate estimation for the inspection cycle 6 months corresponds to $\Delta B_{Insp} = 13.5$ Mt tonnage with the annual accumulated traffic mass $B_j = 27$ Mt/year. The inspection cycle guarantees the reliable fault detection for the middle and long-living individuals (Fig. 1(c)). On the other side, for the long-living crossings, the short inspection cycles are redundant. Therefore the present scheduled inspections system is low appropriate for the common crossings.

Prognostics and health management (PHM) could be a promising concept for the optimization of common crossing inspections and maintenance. The increase of the interest to PHM application in railway transportation by railway companies and by researchers worldwide, can be observed with many recent international projects. The project FASTRACK (Cañete *et al.* 2019) presents sensor platform Sensor4PRI for monitoring of slab track that is developed and tested on Spanish Railways. Multiple acceleration, inclination and distance sensors are integrated to wireless sensor networks, which sends the measurement data to the receiver in the rolling stock. An automatic vision based condition monitoring approach for S&C is presented in (Tastimur *et al.* 2016). A wireless system for the monitoring of sleeper vibrations is introduced in the study (Brajovic *et al.* 2014). The system is used for the evaluation of sleeper deflections and the vertical track stiffness of railway track. An autonomous system that is based on the sleeper acceleration monitoring for S&C, is tested on German (DB) and Swiss Railways (SBB) (Böhm and Weiss 2017). A monitoring of railway track ballast on the lines of French railway company (SNCF) is performed with test sections that includes anchored displacement sensors, accelerometers and extensometers, temperature and humidity sensors (Khairallah *et al.* 2019). An autonomous stress and temperature control system that is tested on Russian Railways (RZhD) is used to detect the danger of track buckling or rail breakage in the continuous welded track (Akkerman and Skutina 2017). An identification of a crossing nose 3D cracks with X-ray tomography is proposed in the project INTELLISWITCH (Dhar *et al.* 2017). A real-time optical fiber monitoring and positioning, is tested on heavy-haul railways of China Railways (He *et al.* 2019). The similar technique is presented in (Minardo *et al.* 2014) for integrated monitoring of railway infrastructures. There are many other monitoring systems, but their wide application by railway companies depends on the reliability and economic efficiency of the monitoring method. In this respect, the most simple, reliable and cost effective solution offer the inertial measurements.

The current study deals with the inertial monitoring of common crossings on DB with the system ESAH-M (*German*: Elektronische System-Analyse im Herzstückbereich – Mobile, *English*: Electronic Analysis System of Crossing – Portable) (Zoll *et al.* 2016). Fig. 2(a) demonstrates the measurements with the system ESAH-M on a common crossing and the measurement device. The device consists of 2 proximity sensors for wheel detection and 3D accelerometer that is installed on the web of frog rail. The proximity sensors are installed on the wing rail and are used for wheel velocity measurement and impact position determination.



(a) ESAH-M system and measurement device



(b) RCF initiation of the frog nose



(c) frog nose RCF damage

Fig. 2 A common crossing monitoring with track side measurements

The principal advantage of the ESAH-M system against the conventional visual and MP inspections is that the system estimates the reason of RCF damages – the dynamic loading of common crossing. Therefore, the measurements allow early detection of RCF deterioration, long before the first visual damages appear. For that matter, the application of the inertial measurements would be promising technique for the optimization of common crossing inspections. Figs. 2(b) and 2(c) show the initiation of RCF cracks on the frog nose and the following spalling damage.

However, the application of inertial measurements for PHM of common crossings is faced with problems of measurements interpretation. The track-side inertial measurements are relatively difficult to interpret, contrary to the engineering problems where the inertial monitoring is successfully used, like gear-box or rolling bearing PHM (Qin *et al.* 2017). The systematic changes in measurement parameters during the lifecycle of bearings (Yin *et al.* 2016) amount to about two orders of magnitude. Whereas the track-side measured accelerations in common crossings have a high random variation that is as high as the systematic changes during the crossing lifecycle (Gerber and Fengler 2007). The performance study (Sysyn *et al.* 2019a) has outlined the reasons of the low signal to noise relation for common crossing monitoring. On the one side, the variation is caused with a lot of unknown factors influencing the measurement results: different train types and their velocities, wheel profile wear, wheel trajectory variation owing to the lateral wheel position, etc. On the other side, the mean accelerations measured at the lifecycle beginning are already high due to initial structural irregularity.

A promising way to cope with the problem of data interpretation is the application of data processing and machine learning methods. A comprehensive overview of modern statistical learning approaches for railway track application is provided in (Attoh-Okine 2017). The study (Sysyn *et al.* 2019b) presents on-board inertial measurements on common crossings for the recent fault detection by means of spectral feature extraction, selection and classification. An application of the statistical and mechanical approaches for the ESAH-M measurements is shown in (Sysyn *et*

al. 2019c), where the reasons of RCF are studied and the crossing lifetime is predicted. A monitoring and prognosis of the track substructure quality development for transition areas from ballastless to ballasted track is presented in (Izvolt *et al.* 2016, Izvolt *et al.* 2017). A development of common crossing diagnosis system with the optimization of the crossing longitudinal profile is proposed in (Kovalchuk *et al.* 2018a, Kovalchuk *et al.* 2018b).

A scale modelling of on-board inertial measurement system with subgrade failure modelling and measurement is shown in (Rapp *et al.* 2019). An application of empirical mode decomposition analysis with linear and non-linear machine learning methods is proposed in (Sysyn *et al.* 2019d) for prediction of common crossing deterioration. A development of track quality indicator that is based on a modified Karhunen–Loève transformation is considered in the study (Chudzikiewicz *et al.* 2018). The algorithm extracts the principal dynamics components from the inertial on-board measurement data. A numerical modelling of common crossing geometry deterioration in comparison with the results of on-board monitoring is presented in (Sysyn *et al.* 2019e). An improvement of the irregularity location estimation with the differential evolution technique and axle box measurements is presented in the paper (Chellaswamy *et al.* 2018). A development of condition indicator for track-side measurements that is based on extraction of time-domain and frequency-domain features, with application of partial least square regression, is shown in (Sysyn *et al.* 2019f). A method of prediction of rail contact fatigue on crossings is proposed in (Sysyn *et al.* 2019g). The method is based on image processing of MP images and machine learning methods. An application of supervised learning methods for rolling noise prediction during railway vehicle operation is presented in (Jeong *et al.* 2019). The prediction is based on survey of rail surface roughness data. A fusion of track settlement on-line data with a physics-based track degradation model is proposed for geometry deterioration prognostics in (Chiachío *et al.* 2019). The prognostics methodology provides accurate predictions of the remaining useful life and is grounded on a filtering-based prognostics algorithm. The paper (Mishra *et al.* 2017) proposes a particle filter-based prognostic approach for railway track switches geometry degradation. The advantage of the approach is better prediction than that of regression approach for longer prediction times as well as its ability to generate a probabilistic result based on input parameters with uncertainties. Point estimate method in comparison with common Monte Carlo simulations for track degradation and track condition modeling are demonstrated in (Neumann *et al.* 2019). The study presents the advantages of point estimate method for cases of complex models or large-scale applications and with only a few specific sample points.

The goal of the present study is improving the scheduled inspections system for common crossings using the data driven RUL prognosis. Thereby, it is considered that the RUL limiting failure mode is RCF damage. The other failure modes, like rail wear, sleeper and fastening damages, ballast settlements etc. could play role for long-living crossings.

2. Preliminary analysis and SE features extraction with MODWPT

The goal of feature extraction is the transformation of the measurement signal into the numerical representation of the signal content that maximizes the recognition of the relevant features. Various techniques are traditionally used for the feature extraction from time series: short time Fourier transform, continuous and discrete wavelet transform (CWT, DWT), maximum overlap DWT (MODWT), wavelet packet transform (WPT), empirical mode decomposition (EMD), multifractal analysis (MFA) (Hoelzl 2019, Zhou and Liu 2019, Landgraf and Hansmann

2018). The DWT enables a time-frequency decomposition of the signal, however the frequency resolution in the DWT is usually considered too coarse for practical analysis in time-frequency domain. CWT is well-suited for the localizing with good resolution the time-frequency features in the signal. However, an aperiodic shift in the time series leads to a different wavelet spectrum that demands the location of transient features on the wavelet spectrogram. WPT is considered as a compromise between the CWT and the DWT that provide a computationally-efficient way with better frequency resolution. MODWT is the stationary version of DWT meaning that the signal compression only occurs in the frequency domain, while the time domain is not down sampled. The good feature of the MODWT for time series analysis is that it divides the data variance by scale. The MODWT, MFA, DWT and CWT have found an application for the data driven degradation evaluation of railway superstructure and substructure and the demand on predictive maintenance (Hoelzl 2019).

The present study exploits the maximal overlap discrete wavelet packet transform (MODWPT) as an appropriate tool for feature extraction from complex signal of common crossing inertial measurements. The MODWPT preserves the signal energy that is an important property which is difficult to realize with conventional bandpass filtering. It is performed with partitioning the energy among the wavelet packets at each level so that the sum of the energy over all the packets equals the total energy of the input signal.

The initial information for the feature extraction and the statistical processing are the track-side inertial measurements and the impact position measurements on the common crossing over its overall lifecycle 29 Mt. The lifecycle is limited by RCF defects that first appeared as the visual surface cracks at about 24-26 Mt. The common crossing with rails UIC60 of steel R350 was installed in the railway turnout with ratio of inclination 1/12 and branch radius 500 m. The operational loading of common crossing is 27 Mt with mixed freight and passenger traffic and velocities 50-160 km/h. Overall monitoring statistic consists of 65 time series that corresponds to separate trains' passages each containing 3 components of acceleration. The measurements were carried out in 11 days uniformly distributed over the lifecycle.

As preliminary analysis, the comparison of similar acceleration signals with different lifetime is performed for estimation of the lifecycle influence on the MODWPT extracted features. Fig. 3 shows the vertical acceleration signal fragments for the same rolling stock and almost the same velocity but the different lifetimes: near to beginning (Fig. 3(a)) and near to the end (Fig. 3(b)).

The comparison of acceleration signals with different lifetimes shows the low difference in the maximal acceleration values. The peak to peak value are almost the same in range about ± 200 g, but the negative acceleration for the old crossing has on average 20 g higher amplitude than the new one. The MODWPT analysis was performed to find out the difference in spectral features between the two cases. The result of MODWPT is an array of coefficients that it is hard to use as features. Therefore these coefficients are reduced to a lower number of high-level features with energy and entropy measures. Shannon entropy (SE) is widely applied in signal processing, information theory, pattern recognition, etc. The wavelet energy for the k^{th} coefficient of the j^{th} node at i^{th} level is defined as follows (Li and Zhou 2016, Li *et al.* 2019)

$$E_{i,j,k} = \|d_{i,j,k}\|^2 \quad (1)$$

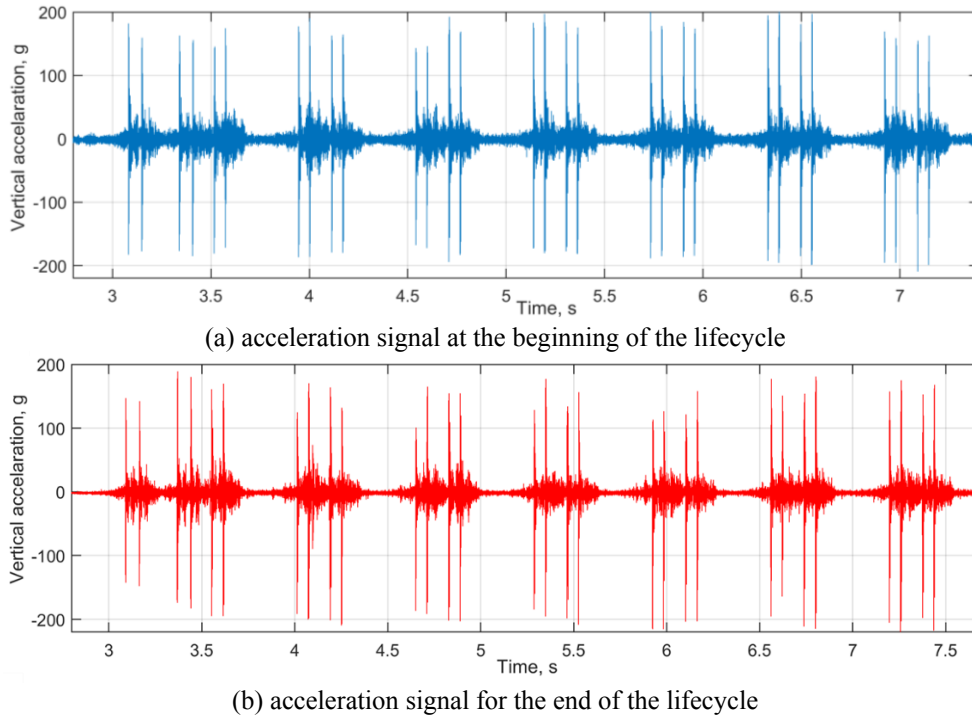


Fig. 3 The vertical accelerations signal fragments in the frog nose of common crossing for trains ICE with velocities about 160 km/h

The total energy for the j^{th} node at i^{th} level can be determined as the sum of the N of the corresponding coefficients in the node

$$E_{i,j} = \sum_{k=1}^N E_{i,j,k} \quad (2)$$

The probability of the k^{th} coefficient for the corresponding node is

$$p_{i,j,k} = \frac{E_{i,j,k}}{E_{i,j}} \quad (3)$$

SE entropy calculated based on the probability distribution of energy

$$SE_{i,j} = -\sum_{k=1}^N p_{i,j,k} \log p_{i,j,k} \quad (4)$$

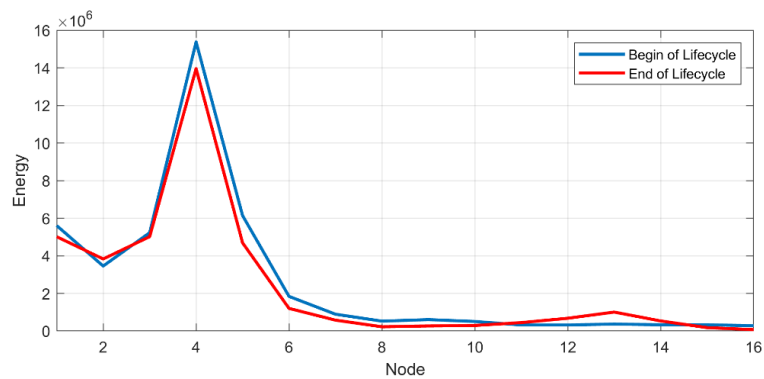
The calculation of MODWPT coefficients is produced with mathematical libraries of Matlab 2019. Fig. 4 presents the results of energy and SE estimation for two cases of acceleration (Fig. 3). The results are presented for 16 nodes. The energy diagram (Fig. 4(a)) shows some difference between the average energy values with the highest relative difference in node 13. Whereas, the SE

diagram (Fig. 4(b)) shows additionally the lines for the partitioned signal to estimate the variance of the parameter. The highest difference between the SE for old and new crossing is in nodes 6, 7, 11, 14-16, however only the nodes 6 and 7 have the clear statistical difference.

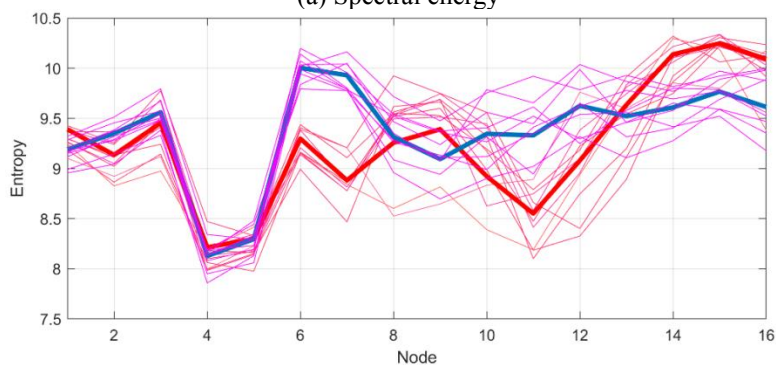
The 16 SE values for each acceleration component are used as the spectral features that are extracted from all measurements. Altogether 50 features are extracted for one measurement that also include the time-domain operational conditions – train velocities and the impact position on the frog nose. The following abbreviations are used to mark the features:

- *seX1-seX16* – SE features for the lateral acceleration;
- *seY1-seY16* – SE features for the vertical acceleration;
- *seZ1-seZ16* – SE features for the longitudinal acceleration;
- *mV* – train velocity;
- *mAP* – impact position on the frog nose.

The signals of accelerations that include the passage of many train axles are partitioned to blocks of width 10000 samples. Thus, the measurement statistic can be expanded from 65 time series to 471 observations. It could be potentially possible to extract number of observations equal to the 2701 passes wheel axles, that would demand the variable partitioning windows due to various train speeds.



(a) Spectral energy



(b) Shannon entropy

Fig. 4 Spectral feature estimates for the new and old common crossing for trains ICE with velocities about 160 km/h

3. The structural health indicator development

The structural health (SH) indicator should provide a good relation to the lifetime of common crossing. Therefore, relevant features should be selected and the redundant or noise features should be rejected before the feature fusion. Additionally, the model of SH indicator should be clear for interpretation, that is important for the practical application. In that regard to this demand, the most suitable model offers the linear regression based methods.

A multiple linear regression model is defined as follows

$$\hat{y}_i = b_1x_{i1} + b_2x_{i2} + \dots + b_px_{ip}, \tag{5}$$

where \hat{y}_i – estimated response; b_p – the fitted coefficients for p -predictor or feature; x_i – the features of i -observation.

The feature selection and regression coefficients b_p calculation is provided with Lasso regularization that identifies important and rejects redundant features. It is performed with a variation of the regularization coefficient λ and the search lowest mean square error in the following formula

$$\min_{b_0, b} \left(\frac{1}{2N} \sum_{i=1}^N (y_i - b_0 - x_i b)^2 + \lambda \sum_{j=1}^p |b_j| \right) \tag{6}$$

where λ – a positive regularization parameter; N – the number of observations; b_0, b – regression coefficients.

The results of the optimal search of shrinkage parameter λ that corresponds to the lowest mean square error is shown on the Fig. 5. The mean square error falls down almost twice with the reduction of the parameter $\lambda_{\min\text{MSE}}$ to the optimal 0.067. The number of considered features grows together with the reduction of parameter λ , as shown on the Fig. 6. Therefore, the optimal number of features is 43 from 50. The optimization is carried out many times according to the 10-fold cross-validation to provide the statistical reliable estimation of the mean square error and their prediction bounds.

The further reduction of parameter λ right from $\lambda_{\min\text{MSE}}$ brings almost no change in the mean square error. The Fig. 5 shows that the λ parameter corresponds to the close to the minimal error values long before the $\lambda_{\min\text{MSE}}$ is achieved. The higher λ corresponds to the lower number of the features selected. It is considered that the low parameter models are more robust than multiparameter one (Hastie *et al.* 2009). Therefore, it would be preferable to choose more robust model if the error increase would be tolerable. The tolerance for the trade-off considers that the increase of deviance is within one standard error relatively to the minimum. The parameter λ for this alternative solution is $\lambda_{1\text{SE}}$ is equal to 0.3 that corresponds to 24 selected features which allow to receive almost the same error as for the optimal 43 features.

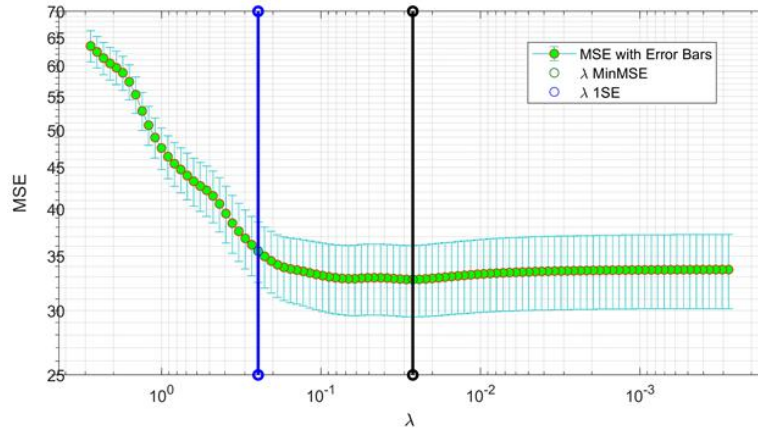


Fig. 5 Mean square error (MSE) in relation to the shrinkage parameter λ

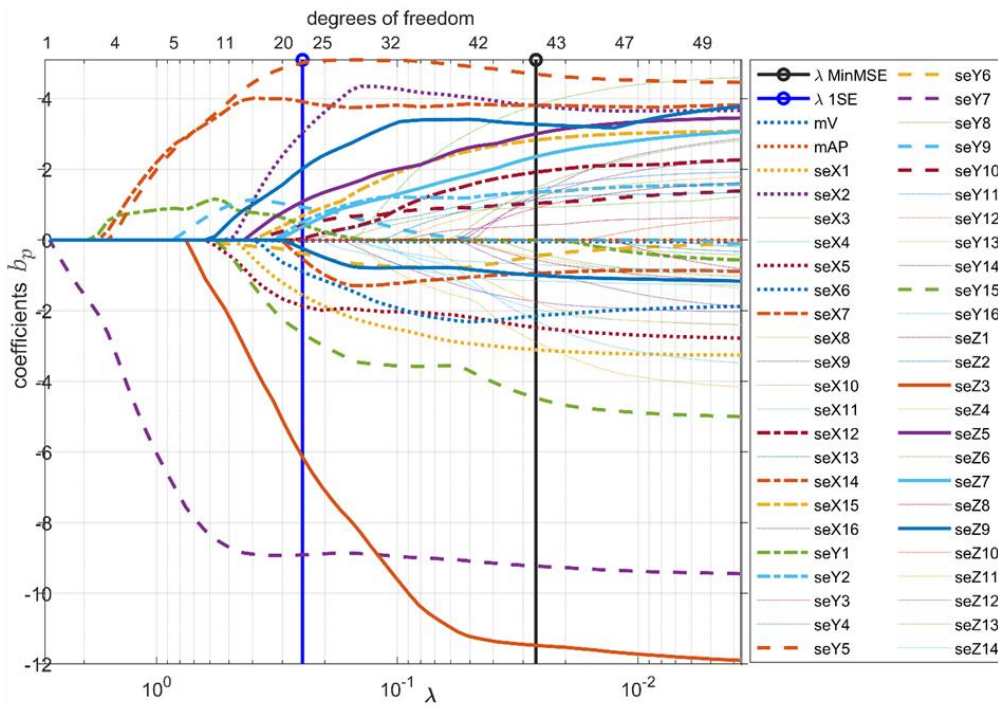


Fig. 6 Lasso regularization plot and optimal number of features

Fig. 6 shows the variation of Lasso regression coefficients b_p that depends on the regularization coefficient λ and the number of selected features. The first left thick lines correspond to the most important features. For higher number of the selected features, more

coefficient lines appear. The thin lines are those that appear right of λ_{1SE} and are considered as redundant.

The feature importance ranking that is shown in the Fig. 7, is derived as the ratio of the coefficient to the mean feature value. The highest influence has the feature of the vertical component of acceleration seY7, that could be good explained with the Fig. 4. Another significant features of the vertical acceleration are seY5 and seY15.

Remarkable is the influence of the feature seZ3 of the longitudinal acceleration component. It could indicate on the changes of the shear dynamic interaction of wheel and rails during the lifetime of crossing. The significant features that are related to the lateral accelerations are seX2 and seX14. The time-domain features mV and mAP have a relatively low influence. That fact could be used for an optimization of the track-side measurement system. The rejection of the wheel proximity measurement could significantly simplify the system.

The data points for the SH indicator that is the estimated response in the formula (5) for the test set are depicted in the Fig. 8. The linear regression demonstrates a good relation of the mean value to the lifetime with narrow function prediction bounds. The developed SH indicator shows much better relation to the lifetime the CWT based indicator, which was developed in the study (Sysyn *et al.* 2019f). The further improvement of the developed SH indicator is possible by combination of the significant time-domain features.

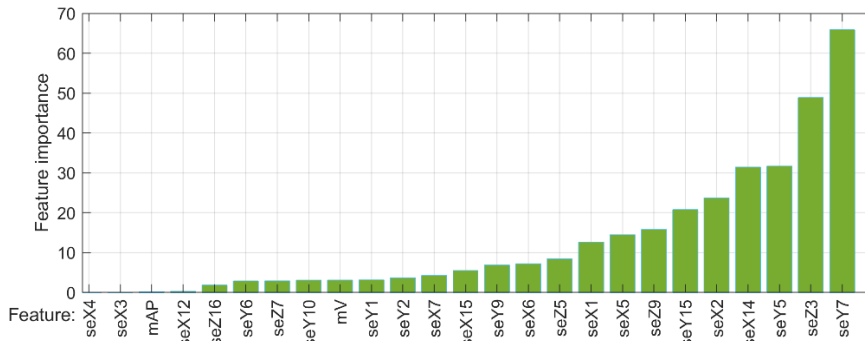


Fig. 7 Feature importance ranking

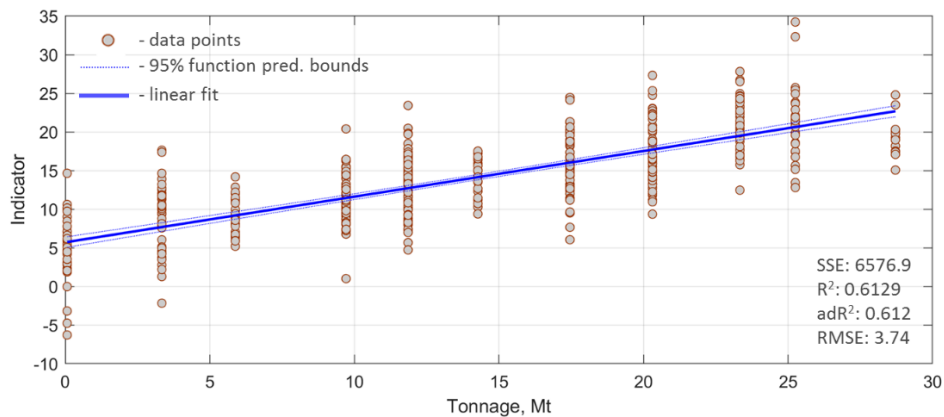


Fig. 8 Linear regression of the SH indicator for 24 selected features

4. Degradation prognosis and remaining useful life estimation

The performed linear regression (Fig. 8) is an exploratory data analysis that explains the relation of SH indicator to the crossing's lifecycle. The estimation of common crossing RUL demands the degradation prognosis that considers only a preceding data available and the prognosis update when the new data comes. The linear degradation model is used to prognose the common crossing degradation, according to the determined linear relation from the last degradation history (Fig. 8). Under the crossing degradation is considered not the specific RCF deterioration, but the increase of inertial loading that does not take into account cumulated damage and mechanical degradation models. The model is based on Wiener process degradation modeling, where stochastic parameters of models are updated via Bayesian approach to incorporate real-time condition monitoring information (Si *et al.* 2017, Kim *et al.* 2017). The estimation of remaining useful lifetime is based on the previous degradation of the system path that is done through the combination of Bayesian updating and expectation maximization algorithm. Linear degradation model is represented with the following formula

$$SHI(t) = \phi + \theta(t)t + \varepsilon(t) \quad (7)$$

where $SHI(t)$ – the condition indicator as a function of time;

ϕ – intercept term considered as known constant;

θ – random parameters determining the model slope, is modeled as a lognormal distribution with mean μ_θ and variance σ_θ ;

t – time step;

$\varepsilon(t)$ – the model additive noise that is modelled as a normal distribution with zero mean and variance $N(0, \sigma^2)$.

At each time step, as the new measured data come, the distribution of model parameters θ , β is updated to the posterior based on the latest observation of SH indicator. The calculation algorithm consists of the following subsequent steps:

1. Bayesian estimation of random parameters θ based on updating the posterior distribution for the parameter via the Bayesian rule;
2. Estimation of the deterministic parameters in $\varepsilon(t)$ based on expectation maximization algorithm;
3. Path-dependent RUL estimation.

The linear degradation model also provides the degradation anomaly detection by the estimation of the slope significance. After a detecting the significant slope of health indicator, the model forgets the previous observations. After that the model restarts the estimation based on the original priors. Figure 9 demonstrates the degradation prognosis after about 50% of the common crossing lifecycle time. The end of life (EoL) of common crossing estimated 29.3 Mt for the accepted threshold of SH indicator 21. The function prediction boundaries provide the uncertainty of prognosis that is ± 2.1 Mt despite of wide deviation range of the observed points.

The prognosis of common crossing degradation and the remaining useful life estimation are complicated with the uncertain SH indicator threshold values. The first visible cracks have appeared at about 23-26 Mt and the rail head spalling after about 28 Mt. Therefore the uncertainty of the lifecycle EoL is about 5 Mt. Figure 10 demonstrates the prognosis quality assessment and the estimation of the necessary inspection time before the corrective action is required. There are many prognostic performance metrics (Saxena *et al.* 2010) like prognostic horizon (PH), α - λ

performance, relative accuracy etc. The metric α - λ performance estimates if the algorithm performs within desired error margins that are specified by the parameter α , of the actual RUL at any given time instant which is specified by the parameter λ . The requirement of the metric is remaining the prognosis within a converging cone of the error margin as a system reaches to EoL.

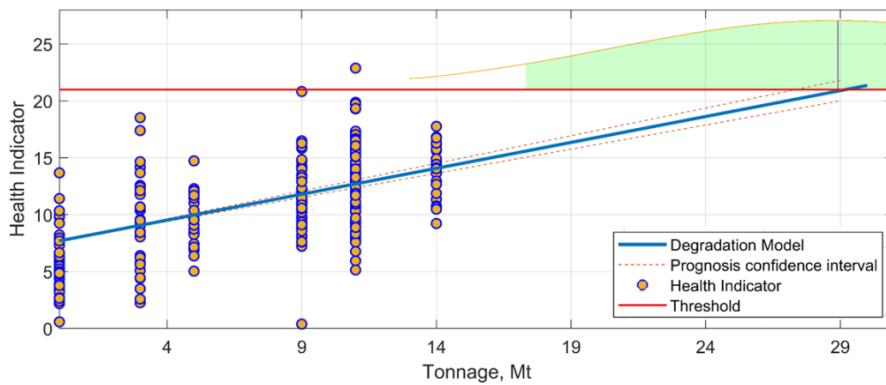


Fig. 9 Common crossing prognosis at 50% of lifetime with linear degradation model

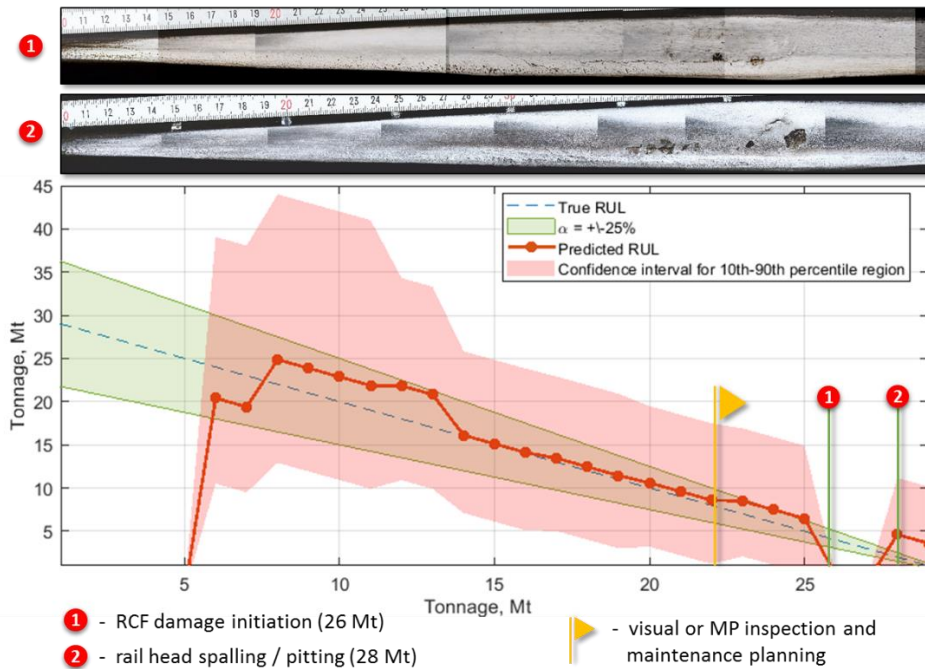


Fig. 10 RUL of common crossing and the inspection time estimation

The present RUL prognosis shows the satisfactory deviation from the true RUL for parameter $\alpha = 0.25$ of the α - λ performance after 6 Mt of the crossing lifetime. The last part of prognosis cannot be taken into account due to the uncertainty of the lifecycle EoL. However, the wide deviation range of the SH indicator points reaches up to half of the lifetime. Taking into account, that the SH indicator is a measure of the inertial loading, whose exceed of the threshold would not lead immediately to the RCF, the observation confidence interval can be limited with 10-90th percentile region. In this case the lower uncertainty bound reaches the EoL after about 22-24 Mt. The time can be considered for the conventional visual inspection or with technical means and the planning of the corrective action after 3-5 Mt.

5. Conclusions

The study has presented an application of PHM approach for the optimization of scheduled inspections for the common crossings. The analysis of the present scheduled inspection system shows the fundamental problems of the interval inspections for the common crossing with high variation of the lifecycles. The possibilities of track-side monitoring techniques are presented for the RCF fault detection and RUL prognosis for the common crossings.

The study has explored the potentials MODWPT analysis for the feature extraction from the inertial measurement signals. The analysis of the SE wavelet features shows much better suitability for recovering the differences between the signals of new and old crossings than the method of conventional maximal acceleration. The applied Lasso regularization selected the best 24 features from extracted 50. The feature importance ranking analysis indicates the significant influence of the features that correspond to the lateral and longitudinal accelerations. The influence of the time-domain features train velocity and the impact position is relatively low. This could be used for an optimization of the measurement system. The developed SH indicator is based on simple linear relation and is simple for the interpretation. RUL prognosis metrics have shown the sufficiently good quality of prognosis. The prognosis enables to plan the visual inspections not more than 5 Mt before the end of lifecycle of common crossing. The proposed PHM approach can reduce the number of time and cost expensive scheduled inspections and at the same time it can reduce the expensive unplanned maintenance works and traffic hindrance. However, the presented approach has also shortcomings that could be handled in further studies. The high variation of SH indicator would need a high number of measurements. An additional improvement of SH indicator with an ensemble of multiple time-domain and spectral indicators would be promising. An application of hybrid approach modelling that takes into account mechanical relations would bring additional improvements.

References

- Akkerman, G.L. and Skutina, M.A. (2017), "Control over transverse shifts of rail sleeper lattice which impact on deformation of ballast layer", *Procedia Eng.*, **189**, 181-185. <https://doi.org/10.1016/j.proeng.2017.05.029>.
- Attoh-Okine, N. (2017), *Big Data and Differential Privacy: Analysis Strategies for Railway Track Engineering*. John Wiley & Sons, Inc., USA. <http://dx.doi.org/10.1002/9781119229070>.
- Brajovic, L.M., Malovic, M., Popovic, Z. and Lazarevic, L. (2014), "Wireless system for sleeper vibrations measurement", *Communications - Scientific Letters of the University of Zilina*, **16**(4), 21-26.

- Böhm, T. and Weiss, N. (2017), "Predictive analytics for railway – monitoring and maintaining point health with smart sensors and AI", *Eisenbahntechnische Rundschau*, **5**, 42-45.
- Cañete, E., Chen, J., Díaz, M., Llopis, L. and Rubio, B. (2019), "Wireless sensor networks and structural health monitoring: Experiences with slab track infrastructures", *Int. J. Distrib. Sens. N.*, **15**(3), 1-16. <https://doi.org/10.1177/1550147719826002>.
- Chudzikiewicz, A., Bogacz, R., Kostrzewski, M. and Konowrocki, R. (2018), "Condition monitoring of railway track systems by using acceleration signals on wheelset axle-boxes", *Transport*, **33**(2), 555-566. <https://doi.org/10.3846/16484142.2017.1342101>.
- Chellaswamy, C., Muthammal, R. and Geetha, T.S. (2018), "A new methodology for optimal rail track condition measurement using acceleration signals", *Measurement Sci. Technol.*, **29**(7), 1-16. <https://doi.org/10.1088/1361-6501/aabe48>.
- Chiachío, J., Chiachío, M., Prescott, D. and Andrews, J. (2019), "A knowledge-based prognostics framework for railway track geometry degradation", *Reliab. Eng. Syst. Safe.*, **181**, 127-141. <https://doi.org/10.1016/j.ress.2018.07.004>.
- Dhar, S., Zhang, Y., Xu, R., Danielsen, H.K. and Jensen, D. (2017), "Synchrotron X-ray measurement of residual strain within the nose of a worn manganese steel railway crossing", *IOP Conference Series: Materials Science and Engineering*, **219**(1), 012016, 38th Risø International Symposium on Materials Science, Denmark, September. <https://doi.org/10.1088/1757-899X/219/1/012016>.
- EU Project INNOTRACK, (2008), *INNOTRACK - Innovative Track Systems*. (Deliverable D3.1.1/D3.1.2, Definition of key parameters and Report on cost drivers for goal-directed innovation), Paris, France. https://cordis.europa.eu/result/rcn/47369_en.html
- Gerber, U., Zoll, A. and Fengler, W. (2015), "Verschleiß und Fahrflächenermüdung an Weichen mit starrer Herzstückspitze [Wear and rolling contact fatigue on common crossings of railway turnouts]", *ETR – Eisenbahntechnische Rundschau*, **01**, 36-41.
- Gerber, U. and Fengler, W. (2007), "Belastung von Weichen mit starrer Herzstückspitze [Load of turnouts with a rigid frog]", *ZEVrail Glaser Annalen*, **131**(5), 202-214.
- He, M., Feng, L. and Zhao, D. (2019), "Application of distributed acoustic sensor technology in train running condition monitoring of the heavy-haul railway", *Optik*, **181**, 343-350. <https://doi.org/10.1016/j.ijleo.2018.12.074>.
- Hoelzl, D. (2019), "Data-driven assessment of railway infrastructure", Master thesis, Institute of Structural Engineering, ETH Zurich, Zurich.
- Hastie T., Tibshirani R. and Friedman J. (2009), *The Elements of Statistical Learning: Data Mining, Inference, and Prediction*, (2nd Ed.), Springer-Verlag, New York, USA.
- Izvolt, L., Sestakova, J. and Smalo, M. (2016), "Analysis of results of monitoring and prediction of quality development of ballasted and ballastless track superstructure and its transition areas", *Communications - Scientific Letters of the University of Zilina*, **18**(4), 19-29.
- Izvolt, L., Sestakova, J. and Smalo, M. (2017), "The railway superstructure monitoring in bratislava tunnel no. 1 - Section of ballastless track and its transition areas", *MATEC Web of Conferences*. <https://doi.org/10.1051/mateconf/201711700063>.
- Jeong, D. and Jeong, W. (2019), "Prediction of rolling noise based on machine learning technique using rail surface roughness data", *J. Korean Soc. Railway*, **22**(3), 209-217. <https://doi.org/10.7782/JKSR.2019.22.3.209>.
- Khairallah, D., Blanc, J., Cottineau, L.M., Hornych, P., Piau, J.-M., Pouget, S., Hosseingholian, M., Ducreau, A. and Savin, F. (2019), "Monitoring of railway structures of the high speed line BPL with bituminous and granular sublayers", *Constr. Build. Mater.*, **211**, 337-348. <https://doi.org/10.1016/j.conbuildmat.2019.03.084>.
- Kovalchuk, V., Sysyn, M., Sobolevska, J., Nabochenko, O., Parneta, B. and Pentsak, A. (2018a), "Theoretical study into efficiency of the improved longitudinal profile of frogs at railroad switches", *Eastern-European J. Enterprise Technologies*, **94**(4), 27-36. <https://doi.org/10.15587/1729-4061.2018.139502>
- Kovalchuk, V., Sysyn, M., Hnativ, Y., Bal, O., Parneta, B. and Pentsak, A. (2018b), "Development of a

- promising system for diagnosing the frogs of railroad switches using the transverse profile measurement method”, *Eastern European Journal of Enterprise Technologies*, **92**(2), 33-42. <https://doi.org/10.15587/1729-4061.2018.125699>
- Kim, N.H., Choi, J.H. and An, D. (2017), *Prognostics and Health Management of Engineering Systems: An introduction*. Springer International Publishing, Switzerland.
- Lichtberger, B. (2005), *Track Compendium: Formation, Permanent Way, Maintenance, Economics*. Eurailpress, Hamburg, Germany.
- Lay, E. and Rensing, R. (2013), *Weichen [Railway Turnouts]*. In Fendrich, L., and Fengler, W., (Eds.), *Handbuch Eisenbahninfrastruktur [Field Manual Railway Infrastructure]* (Vol. 2, pp. 239–306). Springer-Verlag, Berlin Heidelberg, Germany.
- Letot, C., Dersin, P., Pugnaioni, M., Dehombreux, P., Fleurquin, G., Douziech, C. and La-Cascia, P. (2015), “A data driven degradation-based model for the maintenance of turnouts: A case study”, *IFAC PapersOnLine*, **28**(21), 958-963. <https://doi.org/10.1016/j.ifacol.2015.09.650>.
- Landgraf, M. and Hansmann, F. (2018), “Fractal analysis as an innovative approach for evaluating the condition of railway tracks”, *Proceedings of the Institution of Mechanical Engineers, Part F: Journal of Rail and Rapid Transit*, 2018. <https://doi.org/10.1177/0954409718795763>.
- Li, T. and Zhou, M. (2016), “ECG classification using wavelet packet entropy and random forests”, *Entropy*, **18**(8), 285. <https://doi.org/10.3390/e18080285>.
- Li, Y., Wang, J., Zhao, H., Song, M. and Ou, L. (2019), “Fault diagnosis method based on modified multiscale entropy and global distance evaluation for the valve fault of a reciprocating compressor”, *Strojniški vestnik - Journal of Mechanical Engineering*, **65**(2), 123-135. <http://dx.doi.org/10.5545/sv-jme.2018.5487>.
- Minardo, A., Coscetta, A., Porcaro, G., Giannetta, D., Bernini, R. and Zeni, L. (2014), “Distributed optical fiber sensors for integrated monitoring of railway infrastructures”, *Struct.Monit. Maint.*, **1**(2), 173-182. <https://doi.org/10.12989/smm.2014.1.2.173>.
- Mishra, M., Odelius, J., Thaduri, A., Nissen, A. and Rantatalo, M. (2017), “Particle filter-based prognostic approach for railway track geometry”, *Mech. Syst. Signal Pr.*, **96**, 226-238. <https://doi.org/10.1016/j.ymsp.2017.04.010>.
- Neumann, T., Dutschk, B. and Schenkendorf, R. (2019), “Analyzing uncertainties in model response using the point estimate method: Applications from railway asset management”, *Proceedings of the Institution of Mechanical Engineers, Part O: Journal of Risk and Reliability*, (Article in press). <https://doi.org/10.1177/1748006X19825593>.
- Qin, L., Shen, X., Chen, X. and Gao, P. (2017), “Reliability Assessment of Bearings Based on Performance Degradation Values under Small Samples”, *Strojniški vestnik - Journal of Mechanical Engineering*, **63**(4), 248-254. <http://dx.doi.org/10.5545/sv-jme.2016.3898>.
- Rapp, S., Martin, U., Strähle, M. and Scheffbuch, M. (2019), “Track-vehicle scale model for evaluating local track defects detection methods”, *Transportation Geotechnics* **19**, 9-18. <https://doi.org/10.1016/j.jrtpm.2016.03.001>.
- Saxena, A., Celaya, J., Saha, B., Saha, S. and Goebel, K. (2010), “Metrics for offline evaluation of prognostic performance”. *Int. J. Prognostics Health Management*, **1**(1).
- Si, X., Zhang Z. and Hu, C. (2017), *Data-Driven Remaining Useful Life Prognosis Techniques: Stochastic Models, Methods and Applications*. Springer Series in Reliability Engineering, Springer-Verlag GmbH, Berlin Heidelberg, Germany.
- Sysyn, M., Kovalchuk, V. and Jiang, D. (2019a), “Performance study of the inertial monitoring method for railway turnouts”, *Int. J. Rail Transportation*, **7**(2), 103-116. <http://dx.doi.org/10.1080/23248378.2018.1514282>.
- Sysyn, M., Gruen, D., Gerber, U., Nabochenko, O. and Kovalchuk, V. (2019b), “Turnout monitoring with vehicle based inertial measurements of operational trains: A machine learning approach”, *Communications - Scientific Letters of the University of Zilina*, **21**(1), 42-48.
- Sysyn, M., Gerber, U., Nabochenko, O. and Kovalchuk, V. (2019c), “Common crossing fault prediction with track based inertial measurements: statistical vs mechanical approach”, *Pollack Periodica*, **14**(2), 15-26.

- <https://doi.org/10.1556/606.2019.14.2.2>.
- Sysyn, M., Nabochenko, O., Kluge F., Kovalchuk, V. and Pentsak, A. (2019d), “Common crossing structural health analysis with track-side monitoring”, *Communications - Scientific Letters of the University of Zilina*, **21**(3), 79-86.
- Sysyn, M., Gerber, U., Gruen, D., Nabochenko, O. and Kovalchuk, V. (2019e), “Modelling and vehicle based measurements of ballast settlements under the common crossing”, *European Transport / Transporti Europei - International Journal of Transport Economics, Engineering and Law*, 71, 1-25.
- Sysyn, M., Gerber, U., Nabochenko, O., Li, Y. and Kovalchuk, V. (2019f), “Indicators for common crossing structural health monitoring with track-side inertial measurements”, *Acta Polytechnica*, **59**(2), 170-181. <https://doi.org/10.14311/AP.2019.59.0170>.
- Sysyn, M., Gerber, U., Nabochenko, O., Gruen, D. and Kluge, F. (2019g), “Prediction of rail contact fatigue on crossings using image processing and machine learning methods“, *Urban Rail Transit*, **5**(2), 123-132. <https://doi.org/10.1007/s40864-019-0105-0>.
- Tastimur, C., Karakose, M. and Akin, E. (2016), “A vision based condition monitoring approach for rail switch and level crossing using hierarchical SVM in railways”, *IJAMEC*, **4**, 319-325. <https://doi.org/10.18100/ijamec.270634>.
- Yin, A., Lu, J., Dai, Z., Li, J. and Ouyang, Q. (2016). “Isomap and Deep Belief Network-Based Machine Health Combined Assessment Model”, *Strojniški vestnik - Journal of Mechanical Engineering*, **62**(12), 740-750. <http://dx.doi.org/10.5545/sv-jme.2016.3694>.
- Zoll, A. (2016), “Werkstoffauswahl für Weichenhetzstücke durch Prüfstandversuche. [Material selection for point frog points through test bench tests.]” Ph.D. Dissertation, TU Berlin, Berlin.
- Zoll, A., Gerber, U. and Fengler, W. (2016), “Das Messsystem ESAH-M [The measuring system ESAH-M]“, *EI-Eisenbahningenieur Kalender*, **1**, 49-62.
- Zhou, Y., Li, Y. and Liu, H. (2019), “Feature Enhancement Method for Drilling Vibration Signal by Using Wavelet Packet Multi-band Spectral Subtraction”, *Strojniški vestnik - Journal of Mechanical Engineering*, **65**(4), 219-229. <https://doi.org/10.5545/sv-jme.2018.5726>.